Supporting Information for "Spatially Resolved Temperature Response Functions to CO_2 Emissions"

Lyssa M. Freese [1], Arlene M. Fiore [1], Noelle E. Selin [1,2]

[1]Massachusetts Institute of Technology, Earth, Atmospheric, and Planetary Sciences

[2]Massachusetts Institute of Technology, Institute for Data, Systems, and Society

Contents of this file

Introduction

Text S1: Green's Function Analysis

Figure S1 shows that the individual model Green's Functions are different if they are diagnosed from the *esm-pi-CO2pulse* versus the *esm-pi-CDRpulse* experiments. This difference could be due to a variety of reasons, including our limitation to only an individual model run (except in the case of CANESM), or non-linearities in the way CO_2 and heat are taken up versus released by the land and ocean. These individual model Green's

---

Functions vary in their ability to reconstruct the temperature response to the *1pctCO*$_2$ experiment (see Figure S2).

We evaluate the difference between the first thirty and final sixty years of ESGR (scaled by the initial emissions size, 100 GtC) in Figure S3. We split the Green's Function into these two time periods based on (Joos et al., 2013)– defining an initial immediate response over the first four years, and a slower response over the following 32 years. We see increased warming in the poles in the later response time period, in contrast to enhanced warming over land areas in the immediate time period of 0-4 years, as has been explored in (Held et al., 2010).

Text S2: Green's Function Sensitivity to the Smoothing Approach

We use a 4th-order polynomial fit to our Green's Function to reduce the role of internal variability. Here we discuss the sensitivity of this fit as compared to other smoothing approaches, and the role of the convolution in smoothing out internal variability.

In order to minimize the impact of this difference in unforced internal variability that arises, we take a number of steps: 1) averaging across multiple models and realizations, 2) smoothing the Green's function with a 4th-order polynomial fit, 3) comparing ESGR to a Green's function diagnosed from a pulse run and just the climatology of the *pi-ctrl*, and 4) comparing internal variability within models to the inter-model spread. Additionally, the process of the convolution itself also reduces the impact of this internal variability, as positive and negative phases can cancel each other out.

We test the sensitivity of our smoothing approach by comparing the 4th-order polynomial fit to five different Green's Functions (a-e): a) a Green's Function diagnosed by using the 100 gigaton carbon (GtC) pulse (*esm-pi-CO2pulse*) and removal (*esm-pi-CDRpulse*) emission simulations and the *pi-ctrl* simulation; b, c, and d) a 5, 10, and 30-year rolling mean Green's Function, and e) Green's Function diagnosed by using the *esm-pi-CO2pulse* and *esm-pi-CDRpulse* emission simulations and the climatology of the *pi-ctrl* simulation. The comparison to the varying rolling means tests the sensitivity of the timescale of our smoothing approach. Using the climatology for the *pi-ctrl* is a potential way to reduce unforced internal variability in the resulting Green's Function, although it can also falsely attribute drift in the *pi-ctrl* as a signal. Figure S6 shows the impact of various timescales for taking the rolling mean and for a 4th-order polynomial fit of the Green's Function. Much of the noise is canceled out in both the 4th-order polynomial and the 30-year rolling mean, but the curve still maintains a similar magnitude and trend. We then test the impact of these differences on the results of a convolution; once convolved with emissions from a $1pctCO_2$ experiment, the spatial temperature change for each of these six Green's Functions are very similar. Figure S7 shows the root mean squared error (RMSE) for predicted temperatures versus the expected temperatures in a $1pctCO_2$ experiment using the temperature change from each of the six Green's Functions. The RMSE is calculated as: $\sqrt{\sum_{i=0}^{N} \frac{(predicted_i - expected_i)^2}{N}}$, where N is the number of years (limited to 90), the predicted values are temperatures from a convolution, and the expected values are temperatures from the multi-model mean CMIP6 $1pctCO_2$ experiment. The global mean RMSE is lowest for a 4th-order polynomial fit, but as seen in Figure S7, they are all within a similar range of values.

To test whether or not the convolution is reducing the noise, we can take the Fourier transform of our global mean ESGR and of the emissions from a multi-model mean *1pct-CO_2* experiment. Because of the convolution theorem, we know that the Fourier transform of the convolution of these functions is equal to the product of their Fourier transforms. Figure S8 shows the Fourier transform of ESGR, where it is clear that there is a strong low-frequency signal, as well as a number of weaker high-frequency signals that indicate either forced or unforced internal variability. The Fourier transform of the function of the emissions similarly has a strong low-frequency signal and very few weak high-frequency signals. The product of these two dampens these higher-frequency signals; since the product of the Fourier transforms is the same as the Fourier transform of their convolution, we can say that the high-frequency noise (internal variability), is being reasonably reduced by the convolution process.

Text S3: Trajectory Creation

We create six trajectories that have the same cumulative emissions as the *1pctCO_2* experiment by the year a global mean 2°C is reached (year 69). These trajectories are meant to exemplify the importance of historical emissions on temperature outcomes, and are idealized smooth power-law fits of emissions that follow the equation:

$$e(t) = \frac{(c(n+1)t^n)}{t_f^{n+1}} \tag{1}$$

scaled such that $\int_{t=0}^{t_f} e(t)dt = c$, where c is the cumulative emissions desired (1204.7 GtC), t is the time range of emissions (0-90 years), t_f is the time by which c is reached (69 years), and n is polynomial fit desired. We calculate the emissions for n = 1/8, 1/4, 1/2, 2, 4, and 8.

References

Held, I. M., Winton, M., Takahashi, K., Delworth, T., Zeng, F., & Vallis, G. K. (2010, May). Probing the Fast and Slow Components of Global Warming by Returning Abruptly to Preindustrial Forcing. *Journal of Climate*, *23*(9), 2418–2427. Retrieved 2023-02-13, from https://journals.ametsoc.org/view/journals/clim/23/9/2009jcli3466.1.xml (Publisher: American Meteorological Society Section: Journal of Climate) doi: 10.1175/2009JCLI3466.1

Joos, F., Roth, R., Fuglestvedt, J. S., Peters, G. P., Enting, I. G., von Bloh, W., ... Weaver, A. J. (2013, March). Carbon dioxide and climate impulse response functions for the computation of greenhouse gas metrics: a multi-model analysis. *Atmospheric Chemistry and Physics*, *13*(5), 2793–2825. Retrieved 2020-12-16, from https://acp.copernicus.org/articles/13/2793/2013/ doi: 10.5194/acp-13-2793-2013

Table S1. Model Information for Green's Function Derivation. *Italicization indicates that the realizations that are in italics only have the Experiment IDs italicized.*

Model	Realizations	Experiment IDs	Data Variables	Frequency	Weighting Function
GFDL	r1i1f1p1	esm-pictrl, esm-pi-CO2pulse, esm-pi-cdr-pulse	tas	monthly	1
NORESM2	r1i1f1p1	esm-pictrl, esm-pi-CO2pulse, esm-pi-cdr-pulse	tas	monthly	1
UKESM1	r1i1f2p1	esm-pictrl, esm-pi-CO2pulse, esm-pi-cdr-pulse	tas	monthly	1
CanESM5	r1i1f1p2, *r2i1f1p2*, *r3i1f1p2*	esm-pictrl, *esm-pi-CO2pulse*, *esm-pi-cdr-pulse*	tas	monthly	1/3, 1/3, 1/3
ACCESS	r1i1f1p1	esm-pictrl, esm-pi-CO2pulse, esm-pi-cdr-pulse	tas	monthly	1
MIROC	r1i1f2p1	esm-pictrl, esm-pi-CO2pulse, esm-pi-cdr-pulse	tas	monthly	1

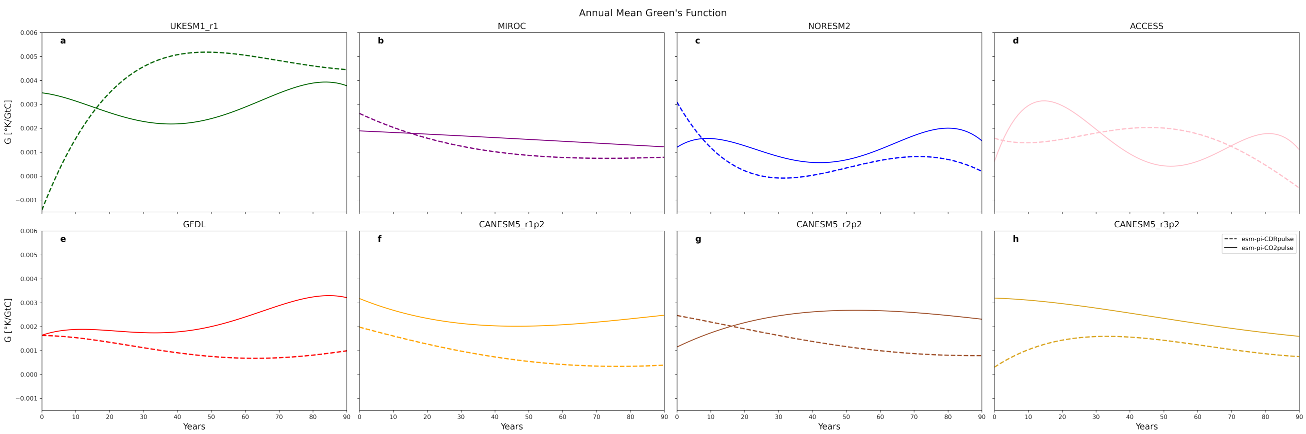

Figure S1. 4th-order polynomial fit global mean Green's Function for every model in both the *esm-pi-CO2pulse* and *esm-pi-CDRpulse*.

Table S2. Model Information for 1pctCO_2 Comparison

Model	Realizations	Experiment IDs	Data Variables	Frequency	Weighting Function
GFDL	r1i1f1p1	pictrl, 1pctCO2	tas, co2mass, fgco2, nbp, areacella	monthly	1
NORESM2	r1i1f1p1	pictrl, 1pctCO2, esm-1pct-brch-1000PgC	tas, co2mass, fgco2, nbp, areacello, areacella	monthly	1
UKESM1	r1i1f2p1, r2i1f2p1, r3i1f2p1, r4i1f2p1	pictrl, 1pctCO2, esm-1pct-brch-1000PgC	tas, co2mass, fgco2, nbp, areacello, areacella	monthly	1/4 1/4 1/4 1/4
CanESM5	r1i1f1p2, r2i1f1p2, r3i1f1p2	pictrl, 1pctCO2, esm-1pct-brch-1000PgC	tas, fgco2, nbp, areacello, areacella	monthly	1/3, 1/3, 1/3
ACCESS	r1i1f1p1	pictrl, 1pctCO2, esm-1pct-brch-1000PgC	tas, fgco2, nbp, areacello, areacella	monthly	1
MIROC	r1i1f2p1	pictrl, 1pctCO2, esm-1pct-brch-1000PgC	tas, fgco2, nbp, areacello, areacella	monthly	1

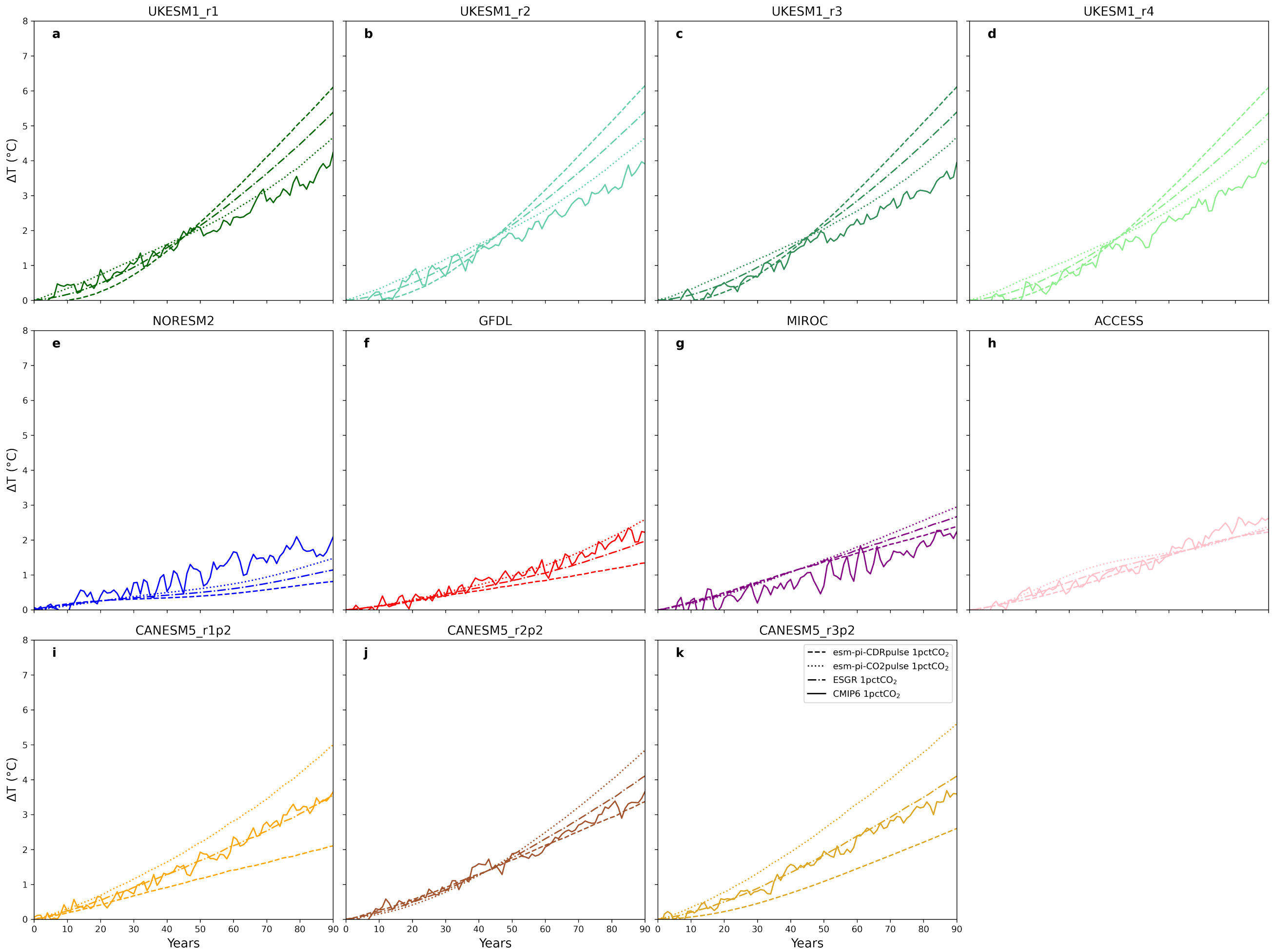

Figure S2. Global mean temperature change in each model for a *1pctCO$_2$* experiment in the CMIP6 model, compared to ESGR and convolutions with the individual pulse types (*esm-pi-CO2pulse* and *esm-pi-CDRpulse*)

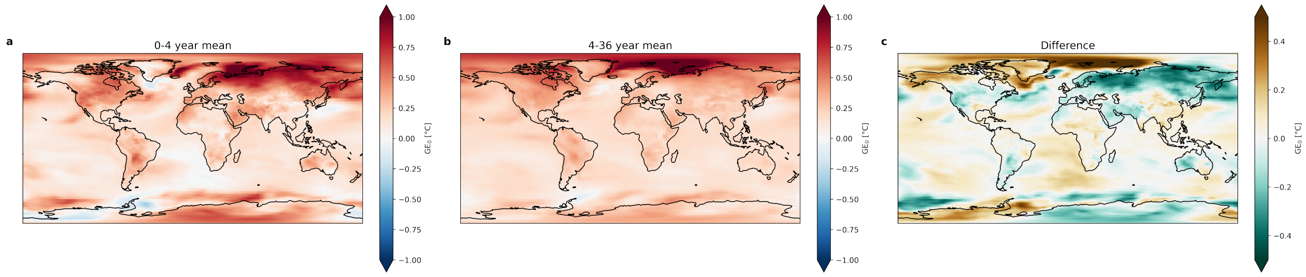

Figure S3. The time-mean ESGR scaled by the initial emissions size of 100GtC between 0-4 years and 4-36 years, and the difference between the two.

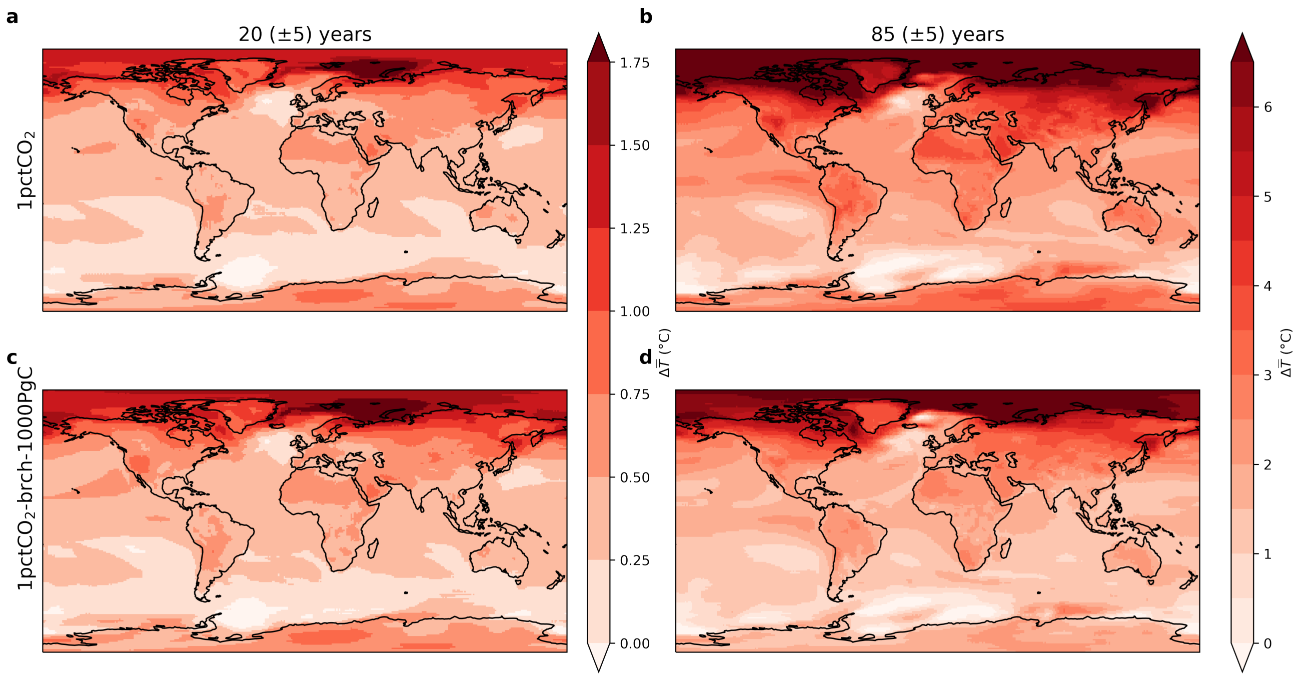

Figure S4. Temperature change in ESGR due to the *1pctCO$_2$* and *esm-1pct-brch-1000PgC* scenarios at 20 (±5) years and 85 (±5) years.

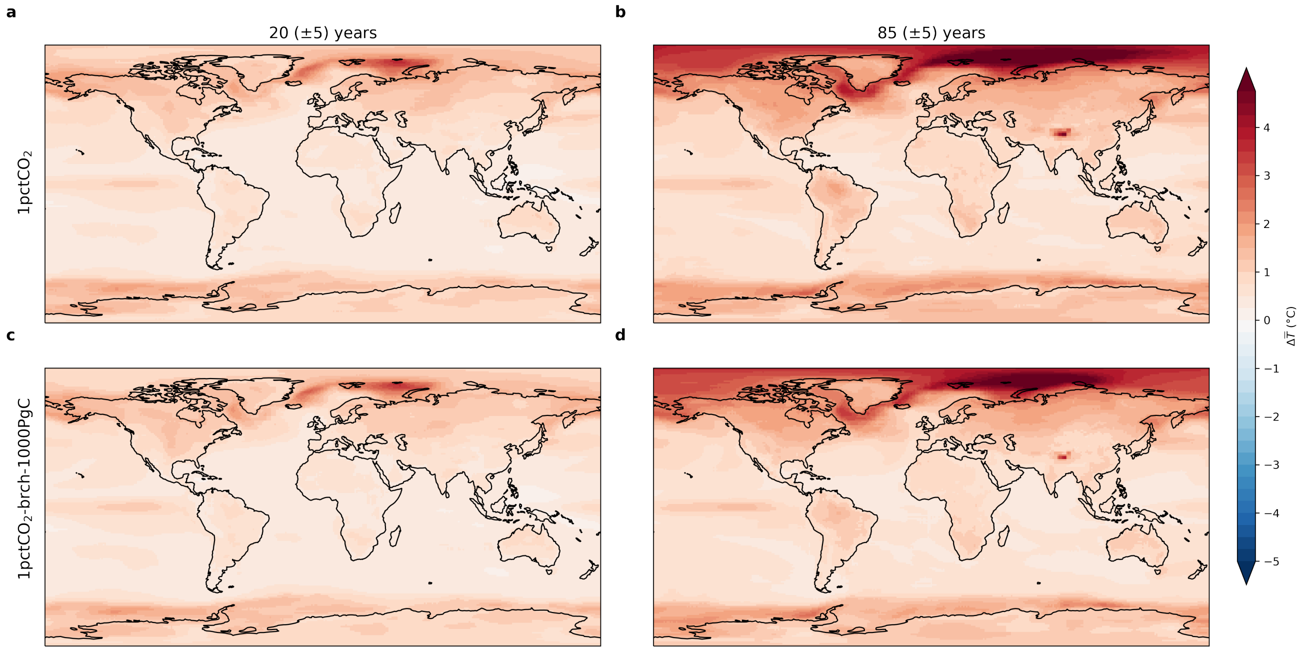

Figure S5. Intra model spread, shown as 1σ as used for determining hatching in S5 at 20 ($\pm$5) years and 85 ($\pm$5) years.

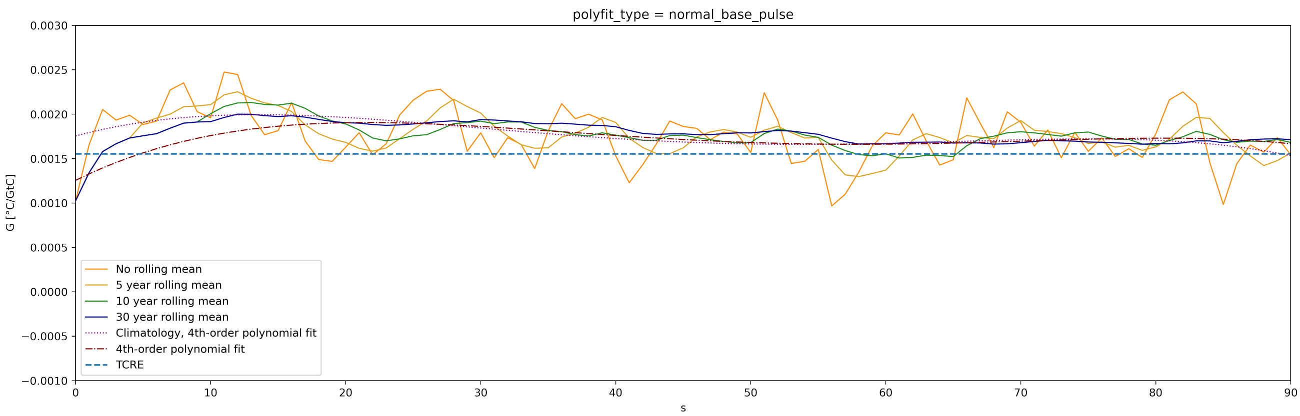

Figure S6. Global mean Green's function for the rolling mean at varying windows (5, 10, 30, and none), the 4th-order polynomial fit, and the 4th-order polynomial fit using a *pi-ctrl* climatology. The dashed line shows the TCRE.

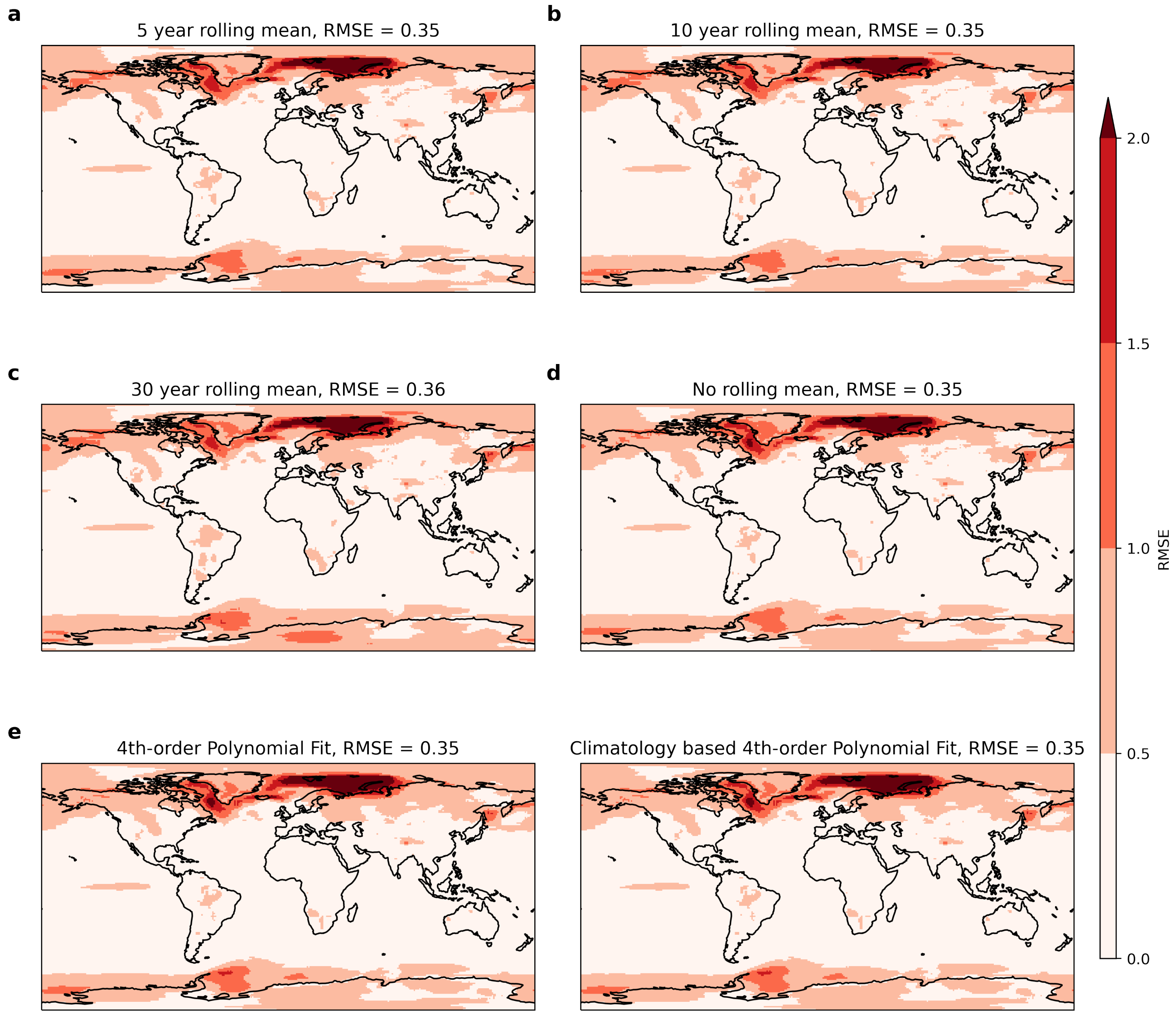

Figure S7. The root mean squared error (RMSE) for temperature change in ESGR compared to the CMIP6 *1pctCO$_2$* multi-model mean. a) shows a 5-year rolling mean ESGR, b) a 10-year rolling mean, c) a 30-year rolling mean, d) no rolling mean, e) a 4th-order polynomial fit, and f) a 4th-order polynomial fit using the *pi-ctrl* climatology.

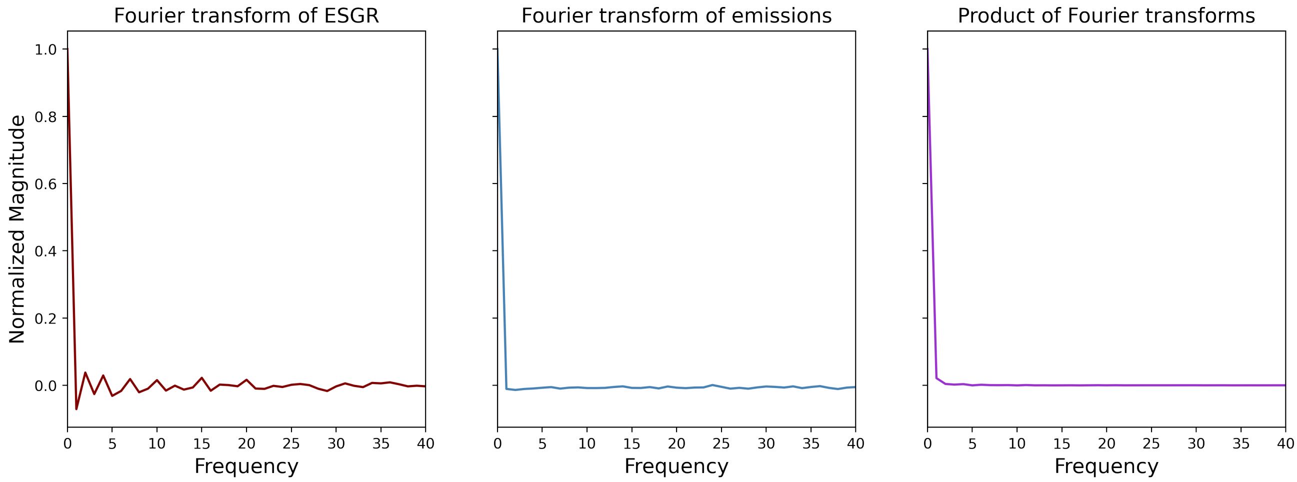

Figure S8. The Fourier transform of the global mean ESGR, the Fourier transform of the emissions from a multi-model mean *1pct-*CO_2 experiment, and their product. All values are normalized to the peak magnitude.